

Exp2VLA: Enabling Vision–Language–Action for Drone Navigation from Expert Demonstrations

1st Van Huyen Dang[‡]
Automatic Control Group
Paderborn University
Paderborn, Germany
van.huyen.dang@upb.de

2nd Kabillesh Rajendran[‡]
Automatic Control Group
Paderborn University
Paderborn, Germany
kabillesh@mail.uni-paderborn.de

3rd Erdi Sayar
Automatic Control Group
Paderborn University
Paderborn, Germany
erdi.sayar@upb.de

4th Erdal Kayacan
Automatic Control Group
Paderborn University
Paderborn, Germany
erdal.kayacan@upb.de

Abstract—Vision-language-action (VLA) models open a new path toward intuitive robot control by directly linking perception, language, and action in a single end-to-end framework. Yet for UAVs, practical adoption remains difficult because existing solutions are either computationally heavy or insufficiently capable in complex environments. In this work, we propose a practical expert-distillation pipeline (Exp2VLA) for language-conditioned drone navigation. The core idea is to distill expert behavior, obtained from reinforcement learning, teleoperation, or other controllers, into training data that can be used to fine-tune compact VLA models. This allows existing control strategies to be transferred into a unified language-guided navigation model, reducing manual system integration and lowering the barrier for deploying new robot behaviors. Experiments in both sim-to-sim and simulation-in-the-loop settings across multi-object scenes show that the fine-tuned models can handle varied semantic commands and generalize to unseen target compositions. The proposed framework demonstrates how expert-policy distillation can help mechatronic systems move from specialized control modules toward more flexible and reusable robot intelligence.

Index Terms—Aerial Robotics, Vision-Language-Action Models, Language-Conditioned Navigation

I. INTRODUCTION

ROBOTIC systems, including aerial robots, operate under diverse physical constraints and environments. Consequently, different platforms require different strategies for perception, decision-making, and control, as well as different mechatronic designs that tightly couple sensing, actuation, and computation.

Recent advances in deep learning offer an alternative paradigm in which robots learn complex behaviors directly from data [1]–[3]. Learning-based approaches can integrate perception and control within unified architectures, reducing reliance on hand-crafted intermediate representations. More recently, vision-language-action (VLA) models (see Fig. 1) have emerged as a promising direction toward more general and flexible robotic systems. These models jointly process visual observations and language instructions to produce robot actions, enabling robots to reason about tasks, environments, and their underlying mechatronic dynamics in a more expressive

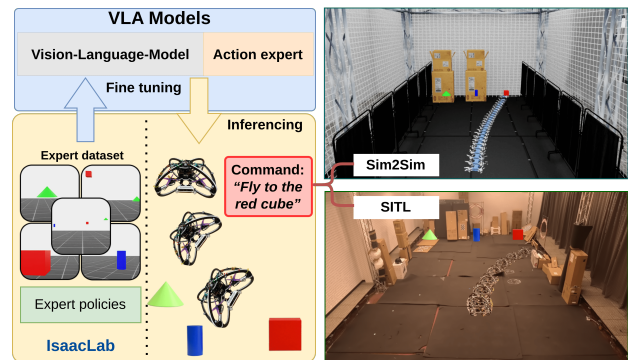


Fig. 1. Overview of the proposed Exp2VLA pipeline. Expert policies in Isaac Lab generate demonstration rollouts, which are converted into a dataset for fine-tuning a vision-language-action model. At inference time, the fine-tuned model takes RGB observations and language commands as input and produces control actions for drone navigation. We evaluate the resulting policy in both sim-to-sim and simulation-in-the-loop (SITL) settings.

manner. Building on the potential of VLA models for complex real-world tasks, we present Exp2VLA, an expert-distillation pipeline for language-conditioned drone navigation. Our approach distills expert behavior into training data for fine tuning a compact VLA model, enabling existing control strategies to be transferred into an end-to-end aerial navigation model. In this way, expert-to-VLA pipeline (Exp2VLA) moves VLA-based drone control closer to practical deployment on resource-constrained platforms.

We summarize our contributions as follows:

- We introduce Exp2VLA, an expert-distillation pipeline that distills expert demonstrations from reinforcement learning, teleoperation, or other controllers into training data for VLA-based drone navigation.
- We integrate expert-driven data collection in simulation, automated conversion to the LeRobot format, and end-to-end policy adaptation into a unified framework for language-conditioned aerial control.
- We validate the proposed approach through both sim-to-sim and simulation-in-the-loop experiments, showing that fine-tuned VLAs with Exp2VLA can follow semantic commands across multi-object scenes and generalize to unseen object-color compositions.

*This work is supported in part by the Horizon Europe Grant Agreements No. 101136056 and No. 101119774.

‡These authors contributed equally to this work.

- We publicly release our datasets to support reproducibility and future research¹.

The paper is structured as follows: Section II summarizes related work, while Section III presents the proposed method. Section IV describes the simulation setup and experimental evaluation, and Section V concludes with insights and directions for future work.

II. RELATED WORK

Recent works have applied VLA models to mobile and embodied robots beyond fixed-base manipulation. For instance, [4] proposes a hierarchical framework for legged robot navigation, in which a VLA model generates mid-level language commands that are executed by a low-level locomotion policy. Similarly, [5] introduces a unified VLA framework for quadruped robots that grounds natural-language instructions into continuous control actions, supported by the MobileVLA-CoT dataset and a two-stage training strategy combining supervised chain-of-thought learning with reinforcement learning. In [6], pre-trained VLA models are adapted from fixed-base manipulators to mobile manipulators using VLA-generated waypoints. Taken together, these studies show that VLA models are increasingly being extended from manipulation toward broader embodied control settings.

This trend naturally motivates the study of VLA-based control for aerial robots. However, transferring these advances to unmanned aerial vehicles (UAVs) is nontrivial because aerial robotics lacks the kind of large-scale, domain-specific demonstration data that has supported progress in manipulation and ground robotics. In particular, datasets capturing expert behavior from first-person flight perspectives remain scarce. As a result, effectively training or adapting VLA models for autonomous UAV operation is substantially more difficult.

Despite these challenges, recent studies have begun to explore VLA-based aerial robotics, although most current approaches rely on large-scale architectures such as OpenVLA-7B [7]. For example, CognitiveDrone [8] introduces a dedicated VLA framework for UAVs that maps first-person visual observations and language instructions directly to continuous control commands through explicit vision–language reasoning modules. AutoFly [9] further extends this direction to autonomous outdoor navigation with a two-stage training strategy and reports both simulation and real-world results. Likewise, RaceVLA [10], one of the first VLA systems designed for high-speed autonomous drones, generates linear and angular velocity commands from first-person-view imagery and language input, but still requires OpenVLA-scale models running on a stationary computer via a network interface. These works establish the feasibility of language-conditioned aerial control, but they also highlight the practical cost of relying on large models.

¹Datasets are available at <https://huggingface.co/datasets/UPB-RAT-VLA/Exp2VLA-SingleCube-v1> and <https://huggingface.co/datasets/UPB-RAT-VLA/Exp2VLA-MultiObject-v1>.

A closely related line of research can be found in recent UAV vision-language-navigation (VLN) systems, which likewise push toward language-grounded aerial autonomy. In UAV-VLN [11], end-to-end language-guided UAV navigation with cross-modal grounding is studied, while VLFly [12] emphasizes open-vocabulary goal understanding for instruction-conditioned flight. The unified aerial VLN framework in [13] further shows that strong navigation performance can be achieved using monocular RGB observations and prompt-guided multi-task learning. While these studies demonstrate rapid progress in language-conditioned aerial navigation, they are primarily formulated as VLN systems rather than compact end-to-end VLA control policies for high-frequency closed-loop deployment.

This raises the question of what model scale is most suitable for deployable aerial VLA systems. Although recent compact VLA models aim to reduce inference cost while retaining multimodal reasoning, sub-billion-parameter architectures such as SmolVLA [14] often lack sufficient capacity for complex spatial reasoning in multi-object scenes with longer temporal horizons. At the other extreme, 7B-class models deliver strong semantic reasoning but typically exceed the computational budgets of edge-deployed UAV platforms. The $\pi_{0.5}$ architecture represents a promising middle ground. Built on the 3B-parameter PaliGemma vision–language backbone with a dedicated 300M-parameter Flow Matching action expert, it supports high-frequency reactive control while preserving strong semantic reasoning and cross-embodiment generalization [15]–[17].

Nevertheless, compact and mid-scale VLA architectures remain largely unexplored in aerial robotics. Most existing UAV-oriented VLA systems still rely on large-scale models, leaving open the question of whether smaller multimodal architectures can provide sufficient reasoning capability while remaining practical for resource-constrained UAVs. Addressing this question requires understanding how multimodal reasoning scales with model size, how limited aerial demonstration data can be leveraged effectively, and how real-time closed-loop control can be maintained under strict computational constraints. These open issues motivate a systematic investigation of compact VLA architectures tailored to aerial deployment.

III. METHODOLOGY

We propose an end-to-end framework for robotics that can gather expert demonstrations from diverse sources, including manual teleoperation, optimal control strategies, and well-trained policies in simulation, and converts them into structured datasets. These datasets enable the fine-tuning of VLA models such as SmolVLA and $\pi_{0.5}$, allowing them to be adapted to a wide range of robotic tasks and platforms. The overall pipeline, illustrated in Fig. 2, is referred to as Exp2VLA.

A. Expert data collection

While the collection of expert demonstrations in our pipeline is inherently agnostic to the underlying control

scheme, accommodating classical control, human teleoperation, or learning-based policies, we opt for an automated approach. Specifically, to establish a robust pre-trained expert for demonstration collection, we train a continuous-control navigation policy using the proximal policy optimization (PPO) [18] algorithm via the RLGames framework [19] within Isaac Lab [20]. The resulting policy serves as an oracle, receiving explicit spatial goal coordinates to guide the agent (UAV) toward visually defined targets (e.g., colored objects). The goal is set at 0.5m offset in front of the visual target to aid in fine-tuning of the VLA models. Once trained, this goal-directed expert is executed in the simulation environment to systematically record high-quality demonstration data across multiple episodes.

At every control step, the following quantities are recorded:

- an RGB frame $\mathbf{I}_t \in \mathbb{R}^{H \times W \times 3}$ (with $H = 480$, $W = 640$) from the drone’s forward-facing camera,
- the drone state vector $\mathbf{s}_t \in \mathbb{R}^6$ comprising linear and angular velocities in body frame,
- the continuous velocity action $\mathbf{a}_t \in \mathbb{R}^3$ executed at that step, including forward (v_x) and vertical (v_z) velocities, and yaw rate ($\dot{\psi}$).
- a natural-language task instruction ℓ_t specifying the desired behavior (e.g., Fly to the red cube), which is tokenized into a numerical representation using the model’s native tokenizer to facilitate multimodal integration.

Data collection spans two environment variants of increasing complexity: single-object scenes and multi-color heterogeneous scenes (see Section IV-A) to expose the policy to diverse spatial configurations and varied combinations of object color and shape. We convert the resulting raw data into the LeRobot [21] dataset format to ensure compatibility with standard VLA training and fine-tuning pipelines.

1) *Dataset characteristics:* Table I summarizes the key properties of the curated heterogeneous scene training dataset. The dataset comprises 1,500 episodes with a fixed episode length of 247 steps yielding a total of 370,500 annotated timesteps. Each timestep includes a 640×480 RGB frame encoded with the AV1 codec, a six-dimensional state observation, and a three-dimensional action command, resulting in a compact dataset size of approximately 0.98 GB. Three distinct natural-language instructions are used, corresponding to the three target objects in the heterogeneous scene environment.

Table II reports per-dimension statistics for the observation state and action vectors for two different data sets:

- Dataset 1 (Exp2VLA-SingleCube-v1) belongs to the data set with a single object (which has only red cubes inside).
- Dataset 2 (Exp2VLA-MultiObject-v1) includes different types of objects and different types of colors.

The state statistics reveal that across both datasets, the drone predominantly moves along the forward axis (v_x : mean ≈ 1.23 m/s for Dataset 1 and 1.14 m/s for Dataset 2), with minimal lateral ($v_y \approx 0$) and vertical ($v_z \approx 0$) drift, consistent with the goal-directed nature of the navigation task. Orientation remains nearly level throughout ($\dot{\phi}$ and $\dot{\theta}$

rates ≈ 0), while the yaw rate exhibits moderate variation ($\sigma \approx 0.14$ rad for Dataset 1 and 0.15 rad for Dataset 2) as the drone adjusts its heading toward the target. In the action space, the active dimensions (v_x , v_z , and $\dot{\psi}$) span the full normalized range $[-1, 1]$ in both datasets, indicating diverse control commands. The other potential control dimensions (v_y , pitch, and roll rates) remain unused, reflecting the constrained action manifold of the velocity controller. This effectively reduces the action space to \mathbb{R}^3 , as described in Section III-A.

B. Fine-tuning VLAs with Exp2VLA

We fine-tune existing VLA models on our curated dataset via imitation learning, focusing on the 4B-parameter $\pi_{0.5}$ and the ultra-compact 0.45B-parameter SmolVLA [14]. To maintain high throughput on a single consumer-grade NVIDIA GeForce RTX 4080 Super (16 GB), we use bfloat16 (BF16) numerical precision for model weights and activations, ensuring a stable dynamic range while significantly reducing the VRAM footprint. To further fit the architectures into limited device memory, we enable gradient checkpointing and freeze the vision encoders (e.g., the 400M-parameter SigLIP [22] for $\pi_{0.5}$), focusing updates exclusively on the action prediction modules. This “expert-only” training regime allows the models to specialize in robotic control while preserving the general-purpose semantic knowledge of their frozen backbones. The policies are optimized for 60,000 iterations with a batch size of 16 for $\pi_{0.5}$ and 64 for SmolVLA, and the learning rate is set to 5×10^{-4} with a cosine decay scheduler based on the

TABLE I
SUMMARY OF THE RGB-SHAPES TRAINING DATASET.

Property	Value
Total episodes	1,500
Total timesteps	370,500
Episode length	247 steps (4.94 s)
Image resolution	$640 \times 480 \times 3$
Video codec	AV1
Unique language instructions	3
Dataset size (on disk)	0.98 GB

TABLE II
PER-DIMENSION STATISTICS OF OBSERVATION STATES AND ACTION COMMANDS FOR DATASET 1 AND DATASET 2. VALUES WITH MAGNITUDE BELOW 10^{-6} ARE REPORTED AS 0.

Dim	Name	Dataset 1*				Dataset 2†			
		Mean	Std	Min	Max	Mean	Std	Min	Max
<i>Observation state</i>									
0	v_x	1.2340	0.9560	0	2.0000	1.1354	0.9704	0	2.0000
1	v_y	0.0005	0.0054	-0.0105	0.0105	0.0024	0.0057	-0.0105	0.0105
2	v_z	0.0476	0.1077	-0.5000	0.5000	-0.0006	0.1361	-0.5000	0.5000
3	$\dot{\phi}$	0	0	0	0	0	0	0	0
4	$\dot{\theta}$	0	0	0	0	0	0	0	0
5	$\dot{\psi}$	0.0180	0.1446	-0.2617	0.2617	0.0253	0.1540	-0.2617	0.2617
<i>Action command</i>									
0	v_x	0.2481	0.9666	-1.0000	1.0000	0.1550	0.9860	-1.0000	1.0000
1	v_z	0.2736	0.2573	-1.0000	1.0000	0.2020	0.3610	-1.0000	1.0000
2	$\dot{\psi}$	0.0687	0.5527	-1.0000	1.0000	0.0970	0.5890	-1.0000	1.0000

An interactive visualization of these datasets is publicly available:

* huggingface.co/Exp2VLA-SingleCube-v1

† huggingface.co/Exp2VLA-MultiObject-v1

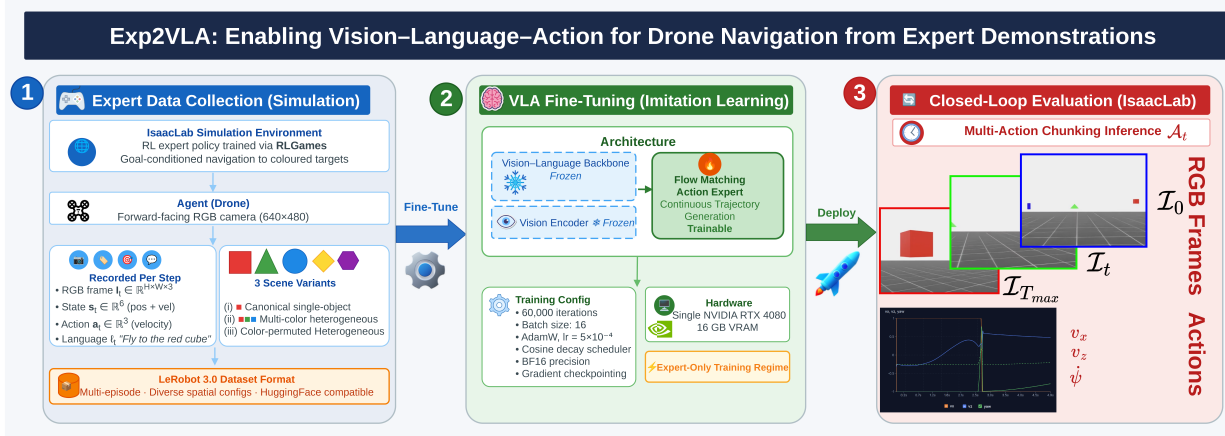


Fig. 2. The Exp2VLA pipeline consists of three stages: (1) collecting expert demonstrations in Isaac Lab and converting them into the LeRobot format, (2) fine-tuning a VLA model via imitation learning, and (3) deploying the fine-tuned models in closed loop for language-conditioned drone navigation in sim-to-sim.

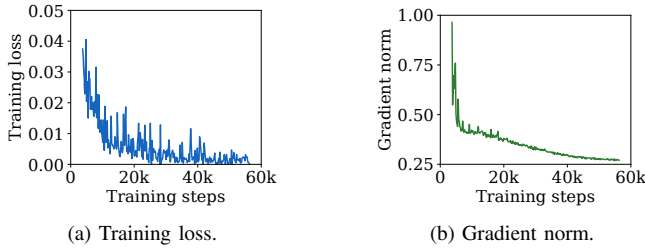


Fig. 3. Training metrics for fine-tuning $\pi_{0.5}$ on datasets obtained via Exp2VLA over 60k steps (batch size 16, $\text{lr} = 5e^{-4}$, BF16 precision). The SigLIP vision encoder is frozen and only the Flow Matching action expert is updated.

total step count. The training loss as well as the gradient norm for the $\pi_{0.5}$ fine-tuning is shown in Fig. 3.

C. Closed-loop evaluation in simulation

The fine-tuned $\pi_{0.5}$ policy is deployed back into Isaac Lab for closed-loop evaluation, following the procedure detailed in Algorithm 1. In each trial, the drone is initialized at a randomized attitude, while target objects are sampled from the position intervals defined in Section IV-A. The model operates exclusively in inference mode: the language instruction is tokenized once at the beginning of the episode, and each inference call receives the latest first-person image, normalized drone state, and fixed language tokens.

To ensure real-time performance and reduce the computational cost of continuous VLA inference, our pipeline utilizes multi-action chunking. Instead of re-inferring at every control timestep, the policy predicts $\mathbf{A}_{t:t+K-1} \in \mathbb{R}^{K \times 3}$, a short sequence of K velocity-style actions corresponding to forward velocity, vertical velocity, and yaw rate. These actions are executed sequentially by the drone controller until the chunk is consumed, the maximum horizon is reached, or the evaluator detects success. An evaluation trial is considered successful if the drone reaches and stabilizes within a predefined distance

Algorithm 1 Closed-loop VLA inference for drone navigation

Require: Policy π_θ , environment \mathcal{E} , command ℓ , target \mathbf{g} , chunk size K , horizon T_{\max} , radius ϵ
Ensure: SUCCESS if the drone reaches \mathbf{g} within ϵ ; otherwise FAILURE

- ▷ Initialize episode and language context
- ▷ State, image, position
- ▷ Fixed command tokens
- while** $t < T_{\max}$ **do**
- ▷ Build observation and infer an action chunk
- ▷ Use training statistics
- ▷ Multimodal observation
- ▷ K actions: v_x, v_z, ψ
- ▷ Execute commands
- for** $k = 0, 1, \dots, K - 1$ **do**
- ▷ Controller command
- $\mathbf{u}_t \leftarrow f_{\text{vel}}(\mathbf{A}_{t:t+K-1}[k])$
- $\mathbf{s}_{t+1}, \mathbf{I}_{t+1}, \mathbf{p}_{t+1} \leftarrow \mathcal{E}.\text{STEP}(\mathbf{u}_t)$
- $t \leftarrow t + 1$
- if** $\|\mathbf{p}_t - \mathbf{g}\|_2 \leq \epsilon$ **then**
- return** SUCCESS
- end if**
- if** $t \geq T_{\max}$ **then**
- break**
- end if**
- end for**
- end while**
- return** FAILURE

threshold ϵ of the target object. Formally, the success condition \mathcal{S} is defined as:

$$\mathcal{S} = \mathbf{1} \left[\min_t \|\mathbf{p}_t - \mathbf{g}\|_2 \leq \epsilon \right], \quad (1)$$

where $\mathbf{p}_t \in \mathbb{R}^3$ and $\mathbf{g} \in \mathbb{R}^3$ denote the drone's position and target coordinates, respectively. Performance is measured by the task success rate across the diverse language-conditioned navigation scenarios.

IV. EXPERIMENTS

A. Experimental setup

All experiments are conducted in Isaac Lab using a quadcopter equipped with a forward-facing RGB camera (640 × 480). The drone operates in a continuous velocity action space. For the evaluated VLA policies, specifically the $\pi_{0.5}$ and SmolVLA backbones, the action chunk size is set to $K = 50$.

At the start of each episode, both the drone and the target are randomized in position to encourage robustness and prevent memorization.

The evaluation success threshold is defined as $\epsilon = 0.60$ m. Specifically, the target object is placed at a random world-frame position with $x \in [5, 7]$ m, $y \in [-2, 2]$ m, and $z \in [0.75, 1.5]$ m relative to the environment origin. The drone is initialized with a randomized altitude $z \in [0.75, 1.5]$ m, while the horizontal position is reset to the environment origin. Each episode lasts 5 seconds, and success is defined by reaching and stabilizing within the acceptance radius ϵ of the commanded object (Eq.1).

To clearly distinguish data collection environments from evaluation conditions, we collect training data in two environments and introduce a third environment exclusively for evaluation. Specifically, we first construct (i) a canonical single-object environment containing only a red cube, which serves as the baseline data collection setting. We then build (ii) a multi-object heterogeneous environment containing three target objects with distinct color-shape combinations: a red cube, a green cone, and a blue cylinder. In addition, to assess generalization beyond the training configurations, we introduce (iii) a color-permuted heterogeneous environment used only for evaluation, in which the same object categories are retained but their color assignments are reassigned to form a green cube, a red cylinder, and a blue cone. Representative onboard camera observations from the two data collection environments are shown in Fig. 4a and Fig. 4b, respectively.

(i) Canonical single-object baseline: A single red cube is placed at randomly sampled positions within a bounded region. The language instruction is fixed to *Fly to the red cube*.

(ii) Multi-color heterogeneous scene: Three objects of varying colors and shapes (red cube, green cone, and blue cylinder) are present simultaneously. The language instruction specifies both color and shape, e.g., *Fly to the green cone*.

(iii) Color-permuted heterogeneous scene: The same three objects are present but the colors are permuted. (green cube, red cylinder, and blue cone). The language instruction again specifies both color and shape, e.g., *Fly to the green cube*.

B. Results and discussion

Tables III, IV, and V report the success rates of our proposed pipeline using the $\pi_{0.5}$ and SmolVLA backbones, denoted as $\text{Exp2VLA}(\pi_{0.5})$ and $\text{Exp2VLA}(\text{SmolVLA})$, respectively. We evaluate both variants in Isaac Lab under closed-loop control across three predefined scenarios: (i) the canonical single-object baseline, (ii) the multi-object heterogeneous scene, and (iii) the color-permuted heterogeneous evaluation scene.

When the evaluation scenarios use the same object-color-shape configurations present in the training dataset (see Fig. 4b), the model consistently demonstrates high performance, achieving a success rate of 68.0% for the red cube, 64.4% for the blue cylinder, and 62.6% for the green cone. The drone’s trajectories for the trained-configuration evaluation

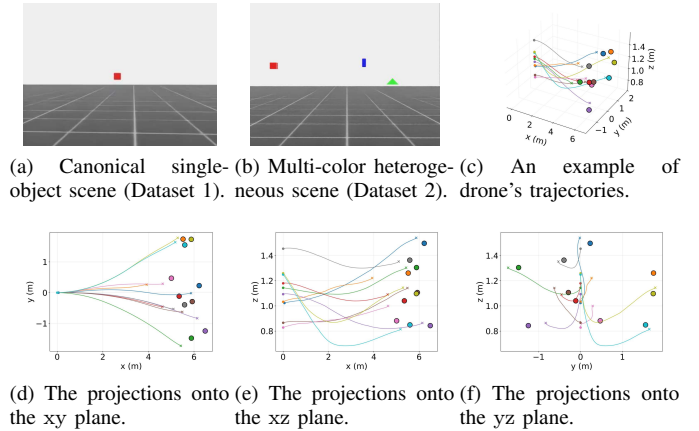


Fig. 4. Training environments: (a) single-object dataset (Dataset 1) and (b) multi-object RGB-shapes dataset with targets varying in color and shape (Dataset 2). (c) Example drone trajectories for *Fly to the red cube* over 10 episodes using $\pi_{0.5}$ backbone. The 3D trajectory is shown with projections onto the xy (d), xz (e), and yz (f) planes. Dots mark start positions, crosses denote final positions, and colored circles indicate target objects.

are visualized in Fig. 4c-4f, which illustrates the drone’s world-frame convergence across 10 evaluation episodes. To assess zero-shot generalization, an additional evaluation was conducted using the color-permuted heterogeneous scene (iii), which contains previously unseen object-color configurations: the object colors were permuted, and the novel command *Fly to the green cube*, *Fly to the red cylinder*, and *Fly to the blue cone* were issued. Although these specific combinations were never encountered during training, $\text{Exp2VLA}(\pi_{0.5})$ maintained an average 51.7% success rate (see Table V), demonstrating robust semantic generalization and the ability to map learned spatial features to novel object-color pairings.

In contrast, comparative evaluations with the $\text{Exp2VLA}(\text{SmolVLA})$ highlight the challenges of deploying ultra-compact VLAs for high-frequency drone control. While the $\text{Exp2VLA}(\text{SmolVLA})$ achieved a 46.6% success rate in Canonical single-object environment (see Fig. 4a and Table III) using configurations seen during training, its performance degraded significantly to 15% in the multi-object RGB-shapes environment (see Fig. 4b and Table IV). This suggests that while such models are efficient, they struggle with the complex spatial-temporal demands and long-horizon requirements of aerial navigation.

To complement the task-success evaluation, we also profile the closed-loop inference time and memory footprint of both backbones. Fig. 5 summarizes the measured inference-loop latency along with the total VRAM usage for each backbone. Although $\text{Exp2VLA}(\text{SmolVLA})$ reduces the total VRAM requirement from 12.90 GB to 6.739 GB, its average loop time is only slightly lower than that of $\text{Exp2VLA}(\pi_{0.5})$. Thus, the practical trade-off is primarily between memory footprint and navigation performance rather than a large latency difference.

Analysis of the results reveals that the performance disparity between $\pi_{0.5}$ and SmolVLA underscores the critical role of vi-

TABLE III
CANONICAL SINGLE-OBJECT SETTING: 500 EPISODES PER TASK, ACCEPTANCE RADIUS $\epsilon = 0.60$ M, AND TARGET OBJECT INCLUDES A SINGLE RED OBJECT ONLY.

Backbone	Target object	Success rate (%)
Exp2VLA ($\pi_{0.5}$)	Red cube	84.10
Exp2VLA (SmolVLA)	Red cube	46.60

TABLE IV
MULTI-COLOR HETEROGENEOUS SCENE: 500 EPISODES PER TASK WITH AN ACCEPTANCE RADIUS OF $\epsilon = 0.60$ M. TARGET OBJECTS INCLUDE A RED CUBE, BLUE CYLINDER, AND GREEN CONE. $\pi_{0.5}$ AND SMOLVLA CONTAIN 4B AND 0.45B PARAMETERS, RESPECTIVELY.

Backbone	Target object	Success rate (%)	Avg. success rate (%)
Exp2VLA ($\pi_{0.5}$)	Red cube	68.00	65.00
	Blue cylinder	64.40	
	Green cone	62.60	
Exp2VLA (SmolVLA)	Red cube	16.00	15.00
	Blue cylinder	14.00	
	Green cone	15.00	

TABLE V
COLOR-PERMUTED HETEROGENEOUS SCENE SETTING: 500 EPISODES PER TASK, ACCEPTANCE RADIUS $\epsilon = 0.60$ M, AND TARGET OBJECT INCLUDES UNSEEN OBJECTS. \dagger ZERO-SHOT EVALUATION ON UNSEEN OBJECTS IN TRAINING.

Backbone	Target objects	Success rate (%)	Avg. success rate (%)
Exp2VLA ($\pi_{0.5}$)	Green cube \dagger	51.0	51.7
	Red cylinder \dagger	75.0	
	Blue cone \dagger	29.0	

sual encoder capacity in enabling effective multi-object aerial navigation. The PaliGemma (3B) backbone in $\pi_{0.5}$ provides sufficiently rich visual-semantic features to distinguish between multiple objects of different colors and shapes, whereas the compact SmolVLA encoder appears unable to maintain discriminative representations when visual distractors are present. Second, the moderate drop in success rate from trained configurations ($\sim 65\%$) to the previously unseen configuration (51.7%) suggests that while $\pi_{0.5}$ has acquired compositional color-shape grounding, this capability remains imperfect—the model can generalize to novel pairings, but not with the same reliability as for configurations encountered during training. Third, the consistent performance across three distinct target objects (red cube, blue cylinder, green cone) indicates that the model does not overfit to a single object type, supporting the effectiveness of the multi-task training strategy with diverse language instructions. Overall, the results indicate that the Exp2VLA($\pi_{0.5}$) architecture provides a favorable balance of reasoning capacity and inference speed, effectively adapting to complex task environments where standard compact VLAs fail to generalize.

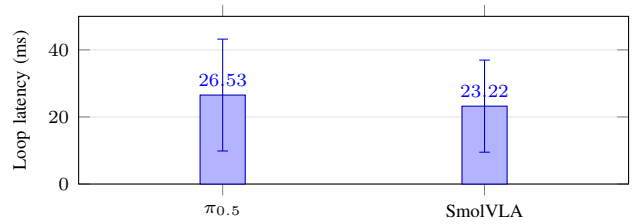
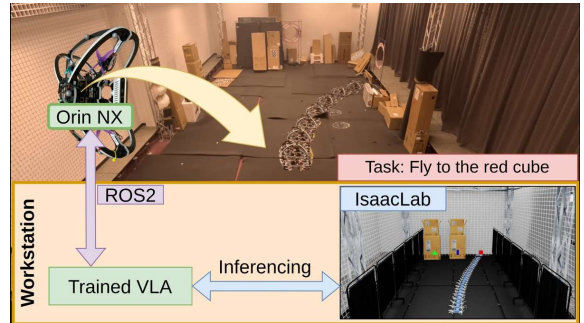


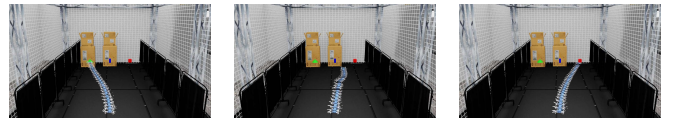
Fig. 5. Measured inference-loop latency for Exp2VLA($\pi_{0.5}$) and Exp2VLA(SmolVLA). Bars show mean loop time with error bars indicating one standard deviation. Exp2VLA($\pi_{0.5}$) requires 12.90 GB VRAM, while the compact Exp2VLA(SmolVLA) requires only 6.739 GB.

C. Simulation in the loop

To demonstrate both generalizability and real-time performance, we first conduct sim-to-sim and simulation-in-the-loop (SITL) experiments. Fig. 6a illustrates the overall SITL pipeline. In the sim-to-sim setup, we build a simulation environment that matches our lab at a one-to-one scale and perform inference on three representative tasks: navigating



(a) The SITL pipeline.



(b) Task: Fly to the (c) Task: Fly to the (d) Task: Fly to the
green cone blue cylinder red cube



(e) Task: Fly to the (f) Task: Fly to the (g) Task: Fly to the
green cone blue cylinder red cube

Fig. 6. The top row (a) presents the SITL pipeline, in which the trained VLA performs inference on a workstation using Isaac Lab and sends commands to the real drone via ROS2. The middle row (b-d) shows sim-to-sim results on three target-reaching tasks, and the bottom row (e-g) demonstrates corresponding real-time executions on the physical platform, highlighting the feasibility of deploying the fine-tuned VLA model in a real-time SITL setting.

to a green cone, a blue cylinder, and a red cube, as shown in Fig. 6b-6d. We then evaluate real-time deployment in an SITL setup, where the trained Exp2VLA($\pi_{0.5}$) is executed on a mobile workstation, since the onboard Orin NX lacks sufficient computational resources to run the full VLA model. The generated control commands are transmitted via ROS2 to the drone in real time. The results in Fig. 6e-6g demonstrate the feasibility of deploying the trained VLA model under this off-board inference configuration.

V. CONCLUSION AND FUTURE WORK

Deploying VLA models on aerial robots remains challenging due to the computational constraints of UAV platforms and the scarcity of domain-specific training data. In this work, we present a lightweight end-to-end pipeline for language-conditioned drone navigation built upon the $\pi_{0.5}$ architecture. Our framework integrates expert-driven data collection in simulation, automated dataset conversion to the LeRobot format, efficient fine-tuning on a single consumer-grade GPU with a frozen vision encoder, and closed-loop evaluation in Isaac Lab. Experimental results show that Exp2VLA($\pi_{0.5}$) achieves up to 68% task success on in-distribution scenarios and maintains 51.7% on zero-shot out-of-distribution configurations involving previously unseen object-color pairings. In contrast, the ultra-compact Exp2VLA(SmolVLA) drops to 15% in multi-object settings, highlighting that sufficient visual encoder capacity is essential for discriminating among multiple targets in complex aerial scenes. The consistent performance across diverse target objects further confirms the effectiveness of multi-task training with varied language instructions. These findings suggest that mid-scale VLA architectures can provide a practical trade-off between reasoning capability and deployment efficiency for resource-constrained aerial platforms.

Future work will improve these models by examining the semantic depth of the action encoders in the interpretation of abstract linguistic cues beyond zero-shot tasks. Additionally, it is essential to address the lack of a standardized common environment for benchmarking drone VLA policies.

ACKNOWLEDGMENT

The authors gratefully acknowledge the funding of this project by computing time provided by the Paderborn Center for Parallel Computing (PC²). This work was partially supported by the Horizon Europe Grant Agreements No. 101136056 and No. 101119774.

REFERENCES

- [1] H. X. Pham, H. I. Ugurlu, J. Le Fevre, D. Bardakci, and E. Kayacan, "Deep learning for vision-based navigation in autonomous drone racing," in *Deep learning for robot perception and cognition*. Elsevier, 2022, pp. 371–406.
- [2] H. X. Pham, A. Sarabakha, M. Odnozhovkin, and E. Kayacan, "Pencilnet: Zero-shot sim-to-real transfer learning for robust gate perception in autonomous drone racing," *IEEE Robotics and Automation Letters*, vol. 7, no. 4, pp. 11 847–11 854, 2022.
- [3] V. H. Dang, A. Redder, H. X. Pham, A. Sarabakha, and E. Kayacan, "Vds-nav: Volumetric depth-based safe navigation for aerial robots—bridging the sim-to-real gap," *IEEE Robotics and Automation Letters*, vol. 10, no. 10, pp. 11 038–11 045, 2025.

- [4] A.-C. Cheng, Y. Ji, Z. Yang, Z. Gongye, X. Zou, J. Kautz, E. Bıyık, H. Yin, S. Liu, and X. Wang, "Navila: Legged robot vision-language-action model for navigation," *arXiv preprint arXiv:2412.04453*, 2024.
- [5] T. Huang, D. Li, R. Yang, Z. Zhang, Z. Yang, and H. Tang, "Mobilevlar1: Reinforcing vision-language-action for mobile robots," *arXiv preprint arXiv:2511.17889*, 2025.
- [6] Z. Wu, Y. Zhou, X. Xu, Z. Wang, and H. Yan, "Momanipvla: Transferring vision-language-action models for general mobile manipulation," in *Proceedings of the Computer Vision and Pattern Recognition Conference*, 2025, pp. 1714–1723.
- [7] M. J. Kim, K. Pertsch, S. Karamcheti, T. Xiao, A. Balakrishna, S. Nair, R. Rafailov, E. P. Foster, P. R. Sanketi, Q. Vuong, T. Kollar, B. Burchfiel, R. Tedrake, D. Sadigh, S. Levine, P. Liang, and C. Finn, "Openvla: An open-source vision-language-action model," in *Proceedings of The 8th Conference on Robot Learning*, ser. Proceedings of Machine Learning Research, P. Agrawal, O. Kroemer, and W. Burgard, Eds., vol. 270. PMLR, 06–09 Nov 2025, pp. 2679–2713. [Online]. Available: <https://proceedings.mlr.press/v270/kim25c.html>
- [8] Z. Huang, Y. Chen *et al.*, "Cognitivedrone: Towards vision-language-action aerial robotics," *arXiv preprint arXiv:2409.06620*, 2024. [Online]. Available: <https://arxiv.org/abs/2409.06620>
- [9] X. Sun *et al.*, "Autofly: Vision-language-action model for uav autonomous navigation in the wild," *arXiv preprint arXiv:2502.01181*, 2025. [Online]. Available: <https://arxiv.org/abs/2502.01181>
- [10] Z. Wang *et al.*, "Racevla: Vla-based racing drone navigation with human-like behaviour," *arXiv preprint arXiv:2503.01245*, 2025. [Online]. Available: <https://arxiv.org/abs/2503.01245>
- [11] J. Dong, Y. Bi, D. Ye, Z. Zhao, Y. Chen, C. Xu, K. Wang, Y. Yang, K. Li, L. Wang, D. Lin, Y. Qiao, H. Fei, and Z. Liu, "Uav-vln: Vision-language navigation for uavs via flight chain-of-thought," *arXiv preprint arXiv:2504.21432*, 2025. [Online]. Available: <https://arxiv.org/abs/2504.21432>
- [12] Y. Ding, R. Zhao, Y. Zhang *et al.*, "Vlfly: Vision-language guided uav navigation in open environments," *arXiv preprint arXiv:2506.10756*, 2025. [Online]. Available: <https://arxiv.org/abs/2506.10756>
- [13] F. Wang, H. Liu, M. Chen *et al.*, "Grounded vision-language navigation for aerial robotics in dynamic environments," *arXiv preprint arXiv:2512.08639*, 2025. [Online]. Available: <https://arxiv.org/abs/2512.08639>
- [14] S. Belkhale, K. Pertsch *et al.*, "Smolvla: A lightweight vision-language-action model for robotic manipulation," *arXiv preprint arXiv:2409.18976*, 2024. [Online]. Available: <https://arxiv.org/abs/2409.18976>
- [15] K. Black, C. Finn *et al.*, " $\pi_{0.5}$: A vision-language-action model with open-world generalization," *Physical Intelligence Technical Report*, 2025. [Online]. Available: <https://www.pi.website/download/pi05.pdf>
- [16] L. Beyer *et al.*, "Paligemma: A versatile 3b vision-language model for transfer," *arXiv preprint arXiv:2407.07726*, 2024.
- [17] X. Zhou, A. Zeng, K. Pertsch *et al.*, "Libero-pro: Towards robust and fair evaluation of vision-language-action models beyond memorization," *arXiv preprint arXiv:2406.08912*, 2024. [Online]. Available: <https://arxiv.org/abs/2406.08912>
- [18] J. Schulman, F. Wolski, P. Dhariwal, A. Radford, and O. Klimov, "Proximal policy optimization algorithms," *arXiv preprint arXiv:1707.06347*, 2017.
- [19] D. Makoviichuk and V. Makoviychuk, "rl-games: A high-performance framework for reinforcement learning," https://github.com/Denys88/rl_games, May 2021.
- [20] M. Mittal, P. Roth, J. Tighe, A. Richard, O. Zhang, P. Du, A. Serrano-Muñoz, X. Yao, R. Zurbrugg, N. Rudin *et al.*, "Isaac lab: A gpu-accelerated simulation framework for multi-modal robot learning," *arXiv preprint arXiv:2511.04831*, 2025.
- [21] F. Capuano, C. Pascal, A. Zouitine, T. Wolf, and M. Aractingi, "Robot learning: A tutorial," *arXiv preprint arXiv:2510.12403*, 2025.
- [22] X. Zhai, B. Mustafa, A. Kolesnikov, and L. Beyer, "Sigmoid loss for language image pre-training (siglip)," in *Proceedings of the IEEE/CVF International Conference on Computer Vision (ICCV)*, 2023.